# A Systematic Survey in Geometric Deep Learning for Structure-based Drug Design

Zaixi Zhang, Jiaxian Yan, Qi Liu, and Enhong Chen

Abstract—Structure-based drug design (SBDD), which utilizes the three-dimensional geometry of proteins to identify potential drug candidates, is becoming increasingly vital in drug discovery. However, traditional methods based on physiochemical modeling and experts' domain knowledge are time-consuming and laborious. The recent advancements in geometric deep learning, which integrates and processes 3D geometric data, coupled with the availability of accurate protein 3D structure predictions from tools like AlphaFold, have significantly propelled progress in structure-based drug design. In this paper, we systematically review the recent progress of geometric deep learning for structure-based drug design. We start with a brief discussion of the mainstream tasks in structure-based drug design, commonly used 3D protein representations and representative predictive/generative models. Then we delve into detailed reviews for each task (binding site prediction, binding pose generation, de novo molecule generation, linker design, and binding affinity prediction), including the problem setup, representative methods, datasets, and evaluation metrics. Finally, we conclude this survey with the current challenges and highlight potential opportunities of geometric deep learning for structure-based drug design.

Index Terms—Geometric Deep Learning, Deep Generative Model, Molecule Generation, Structure-based Drug Design, Survey.

# 1 Introduction

Structure-based drug design (SBDD) [1], [2], [3] is becoming an essential tool to design and optimize drug candidates by effectively leveraging the three-dimensional geometric information of target proteins. Traditionally, the 3D structures of the target protein are obtained with techniques like X-ray crystallography [4], nuclear magnetic resonance (NMR) spectroscopy [5], or cryo-electron microscopy (cryo-EM) [6]. Recently, the progress on high-accurate protein structure prediction such as AlphaFold [7] further boosts the availability of structural data and lays the foundation for its broad applications. SBDD is widely used by pharmaceutical companies and scientists. A number of marketed drugs have been successfully identified with SBDD, such as HIV-1 protease inhibitors [8], the thymidylate synthase inhibitor raltitrexed [9], and the antibiotic norfloxacin [10]. However, traditional structure-based drug design methods that rely on physical modeling, hand-crafted scoring functions, and enumeration are still time-consuming and laborious. To address these issues, geometric deep learning [11] has been recently proposed to speed up and improve the structurebased drug design process.

Geometric deep learning (GDL) [11] are neural network architectures that incorporate and encode 3D geometric data. They can automatically extract informative 3D structural features instead of hand-crafted feature engineering. Furthermore, some GDL methods such as EGNN [12] incor-

Preprint.

porate the symmetry properties into network design as an effective inductive bias for better performance. Symmetry in the context of 3D Euclidean space to rotation, translation, and reflection, and how corresponding protein and molecular properties change under such transformations (more discussions in Sec.2.3). With the rapid development of geometric deep learning, a series of SBDD tasks including binding site prediction [13], binding pose generation [14], *de novo* molecule generation [15], linker design [16], and binding affinity prediction [17] have benefited. Generally, geometric deep learning for SBDD is developing at a fast pace and has drawn more and more attention.

#### 1.1 Differences with Existing Surveys

Given the importance of Structure-based Drug Design, there are a series of published surveys along its development [9], [18], [19], [20], [21], [22], [23]. However, these surveys are from the perspective of biomedicine and chemistry and are published in biomedical or chemical journals, which still brings the domain knowledge barriers to machine learning/deep learning researchers.

Different from existing surveys, this review provides a systematic overview of geometric deep-learning methods for structure-based drug design from the perspective of machine learning/deep learning and is SBDD task-oriented: the sections are organized based on the task categories; each SBDD task is formulated as a machine learning/deep learning problem and the corresponding representative works, benchmark datasets, and evaluation metrics are clearly stated. This will help researchers from the machine learning/ deep learning communities to understand the SBDD tasks with minimal domain knowledge and facilitate them in designing better geometric deep learning algorithms for structure-based drug design.

Zaixi Zhang, Jiaxian Yan, Qi Liu, and Enhong Chen are with the Anhui Province Key Laboratory of Blg Data Analysis and Application (BDAA), School of Computer Science and Technology, University of Science and Technology of China, Hefei, Anhui 230027, China, and State Key Laboratory of Cognitive Intelligence, Hefei, Anhui, 230088, China. E-mail: {zaixi, jiaxianyan}@mail.ustc.edu.cn, {qiliuql, cheneh}@ustc.edu.cn

Correspondence to Qi Liu.

# 1.2 Paper Collection

Since our survey focuses on the interdisciplinary area of geometric deep learning and structure-based drug design, we retrieved the papers from both AI/machine learning top conferences/journals (e.g., NeurIPS, ICLR, ICML, KDD, TKDE, TPAMI) and natural science journals (e.g., Nature, Nature Communications). Meanwhile, we also leveraged Google Scholar to search the recent related works. According to the SBDD tasks that we reviewed in this survey, we used keywords such as structure-based drug design, protein-ligand docking, protein-ligand affinity prediction, linker design, protein binding site prediction, etc, to search the relevant works. Finally, we carefully organized the retrieved papers according to their tasks and methods (see Table. 1).

# 1.3 Organization of This Survey

Firstly in Section 2.2, we briefly introduce the mainstream 3D representations of protein, the SBDD tasks reviewed in this paper, and the popular predictive and generative models. The following sections are organized based on the logical order of SBDD tasks as shown in Figure.1: as for the target protein structure, we first need to identify the binding site; then we can conduct binding pose generation, de novo molecule generation, and linker design; with the proteinligand complex structure, we can use binding affinity prediction and other filtering criteria to filter drug candidates. Admittedly, the order and the category of SBDD tasks are not fixed since SBDD is an iterative process that proceeds through multiple cycles leading optimized drug candidates to clinical trials [24]. Some methods may also be capable of accomplishing multiple tasks. For example, EquiBind [25] can predict the binding pose of ligands without prior knowledge of the binding site, i.e., blinding docking. for the ease of readers' understanding. Finally, Section 4 identifies the open challenges and opportunities, paving the way for the future of designing geometric deep learning methods for structure-based drug design.

# 2 PRELIMINARIES

## 2.1 Overview of SBDD Tasks

In Figure 1, we show the overview of SBDD tasks reviewed in this paper, including binding site prediction, binding pose generation, *de novo* molecule generation, linker design, and binding affinity prediction. Generally, binding site prediction and binding affinity prediction are predictive tasks. The other tasks are generative tasks that are tackled with generative models.

# 2.2 Protein and Ligand Representation

The representation of the protein and ligand molecule depends on the SBDD tasks and the chosen geometric deeplearning methods. In SBDD, proteins are usually characterized by 3D representations to capture critical 3D structural information. The three most prevalent protein representations in recent works are 3D grid, 3D surface, and 3D graph as shown in Figure 2:

 3D grids are Euclidean data structures consisting of regularly spaced 3D elements, i.e., voxels. 3D grids

- have special geometric properties: (1) each voxel has an identical neighborhood structure and is therefore indistinguishable from all other voxels structure wise, and (2) the vertices have a fixed ordering that is defined by the spatial dimensions. Due to the Euclidean structure of the input 3D grid, 3D CNNs are typically applied to 3D grid data for encoding and downstream tasks.
- 3D surface of the protein is defined as the outermost layer of the protein atoms and plays key roles in protein-ligand interactions. Each point on the protein surface can be characterized by the corresponding chemical (e.g., hydrophobic, electrostatic) and geometric (e.g., local shape, curvature) features. From the perspective of data structure, protein surfaces are usually depicted as either a mesh, which is a collection of polygons that outline the surface's location, or as point clouds, which are sets of nodes to represent the surface's location at a specific level of resolution.
- 3D graphs are widely used to represent protein structural data with atoms as nodes and edges as covalent bonds. Edges may also be constructed by connecting the k-nearest neighbors. Geometric Graph Neural Networks [12], [26] are suitable for processing protein 3D graph data.

As for the ligand molecules, their representations vary from 1D string, e.g., simplified molecular-input line-entry system (SMILES) [27] to 2D- or 3D-graphs [28] where nodes represent atoms and edges represent bonds (see Figure 3).

## 2.3 Symmetry

Incorporating the symmetry prior into neural network architectures as inductive bias is proven to be an effective strategy to build generalizable models [11], [29]. The mainstream symmetry groups considered in protein-ligand systems include the Euclidean group E(3), the special Euclidean group SE(3), and the permutation group [11]. Both E(3) and SE(3) include rotation and translation transformations in the 3D Euclidean space. E(3) further covers the reflection operation. Note that SE(3) is applicable when a neural network aims to differentiate chiral systems. Let  $\mathcal T$  denote the transformation,  $\mathcal F$  be the neural network, and  $\mathcal X$  be the input data. The output of the neural network  $\mathcal F(\mathcal X)$  can transform equivariantly, invariantly, or non-equivariantly with respect to  $\mathcal T$ , as defined below:

- Equivariance.  $\mathcal{F}(\mathcal{X})$  is equivariant to a transformation  $\mathcal{T}$  if the transformation of input  $\mathcal{X}$  commutes with the transformation of  $\mathcal{F}(\mathcal{X})$  via a transformation  $\mathcal{T}'$  of the same symmetry group, i.e,  $\mathcal{F}(\mathcal{T}(\mathcal{X})) = \mathcal{T}'\mathcal{F}(\mathcal{X})$ .
- Invariance. Invariance is a special case of equivariance where  $\mathcal{F}(\mathcal{X})$  is invariant to  $\mathcal{T}$  if  $\mathcal{T}'$  is the identity transformation:  $\mathcal{F}(\mathcal{T}(\mathcal{X})) = \mathcal{T}'\mathcal{F}(\mathcal{X}) = \mathcal{F}(\mathcal{X})$ .
- Non-equivariance.  $\mathcal{F}(\mathcal{X})$  is neither equivariant nor invariant to  $\mathcal{T}$  if  $\mathcal{F}(\mathcal{T}(\mathcal{X})) \neq \mathcal{T}'\mathcal{F}(\mathcal{X})$ .

#### 2.4 Predictive Methods

Here we summarize the mainstream predictive methods for predictive tasks, i.e., binding site prediction and binding affinity prediction. These models are also widely used as the structure encoding backbone for generative methods.

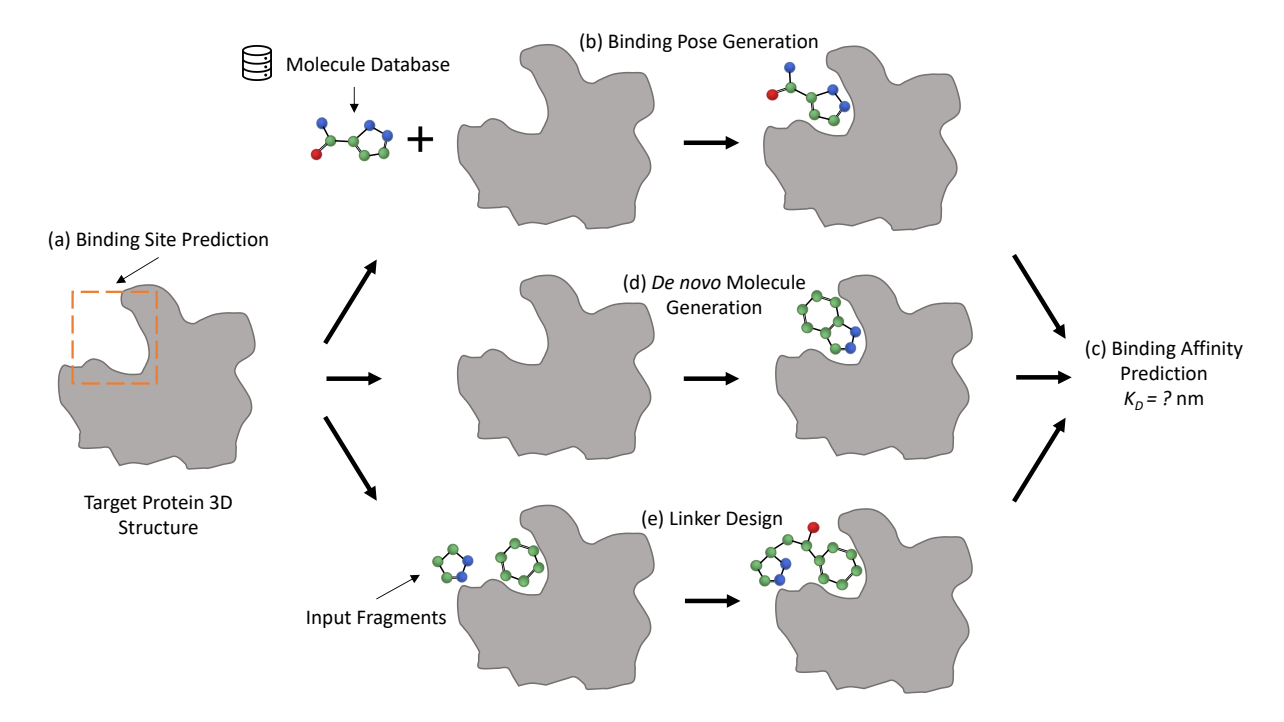


Fig. 1. Structure-based drug design tasks discussed in this survey: (a) Binding site prediction aims to identify areas of the protein structure that can act as binding sites for ligand molecules; (b) Binding pose generation or protein-ligand docking focus on predicting the binding conformations of the protein-ligand complex; (c) binding affinity prediction aims to predict the affinity between a protein and a ligand given their binding structure; (d) *De novo* ligand design generates binding ligand molecules from scratch with the structural information of the target protein; (e) linker design combines disconnected molecular fragments into a combined ligand molecule conditioned on the target protein.

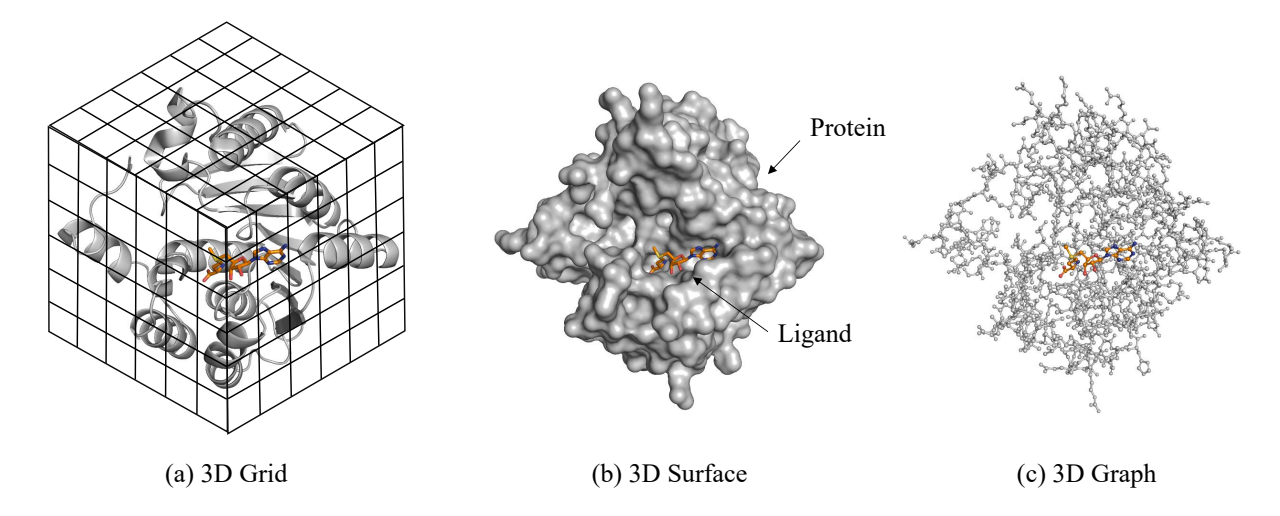


Fig. 2. 3D representations of protein used for geometric deep learning: (a) 3D grid, (b) 3D surface, and (c) 3D graph, illustrated for PDB ID 2avd.

## 2.4.1 Convolutional Neural Networks (CNNs)

CNNs are widely used for image processing where the input elements i.e., pixels are arranged spatially. CNNs rely on the shared-weight architecture of the convolution kernels or filters that slide along input features and provide translation-equivariant outputs. Depending on the data structure, the convolution kernels or filters vary. For example, for the 3D surface data, MaSIF [13] defines geodesic convolutional layers with the geodesic polar coordinates. For the 3D grid data, 3D CNNs are widely used [30], [31].

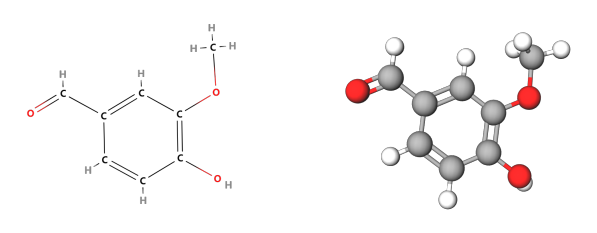
# 2.4.2 Graph Neural Networks (GNNs)

GNNs are widely used to model relational data. Most GNNs follow a message-passing paradigm. Let the  $h_i$  be the node feature of the i-th node in the graph and  $e_{ij}$  be the edge feature for the optional edge connecting node i and j. GNNs iteratively conduct message computation and neighborhood aggregation operations for each node (or edge). Generally, we have:

$$m_{ij} = \psi_m(h_i, h_j, e_{ij}), \tag{1}$$

$$h'_{i} = \psi_{h}(\{m_{ij}\}_{j \in \mathcal{N}(i)}, h_{i}),$$
 (2)

where  $\mathcal{N}(i)$  denote the set of neighbors of node i,  $h_i'$  is the updated node feature, and  $\psi_m, \psi_h$  are learnable functions.



- (a) 2D molecular Graph
- (b) 3D molecular Graph

Fig. 3. Three representations of an example molecule. The 1D SMILES string is COc1cc(C=O)ccc1O; Figures 3(a) and 3(b) are the 2D and 3D molecular graph respectively. 2D and 3D figures are from https://molview.org.

For the 3D structural data, each node in the 3D graph not only has scalar features but also contains 3D coordinates. Equivariant graph neural networks are proposed to incorporate geometric symmetry into model building [32]. Let  $v_i \in \mathbb{R}^3$  denote the 3D coordinate, we have:

$$m_{ij} = \psi_m(\mathbf{v}_i, \mathbf{v}_j, h_i, h_j, e_{ij}), \tag{3}$$

$$\boldsymbol{m}_{ij} = \psi_{\boldsymbol{m}}(\boldsymbol{v}_i, \boldsymbol{v}_j, h_i, h_j, e_{ij}), \tag{4}$$

$$h_i' = \psi_h(\{m_{ij}\}_{j \in \mathcal{N}(i)}, h_i), \tag{5}$$

$$\mathbf{v}_i' = \psi_{\mathbf{v}}(\{\mathbf{m}_{ij}\}_{j \in \mathcal{N}(i)}, \mathbf{v}_i), \tag{6}$$

where  $m_{ij}$  and  $m_{ij}$  are scalar and vector messages.  $\psi_m$  and  $\psi_h$  are geometrically invariant functions while  $\psi_m$  and  $\psi_v$  are geometrically equivariant functions. Compared with traditional 3D CNNs, geometrically equivariant GNNs do not require the voxelization of input data while still maintaining the desirable equivariance. Some representative equivariant GNNs are SchNet [33], EGNN [12], GVP [34], DimeNet [35], [36], GMN [37], SphereNet [38], and ComENet [39].

## 2.4.3 Graph Transformer

Transformer was originally proposed for sequence data [40]. Recently, researchers have successfully adapted Transformer architectures to 2D- and 3D-graph data and achieved superior performance [41], [42], [43], [44], [45]. Typically, a Transformer is composed of stacked Transformer blocks. A transformer block consists of two layers: a self-attention layer followed by a feed-forward layer with normalizations (e.g., LayerNorm [46]) and skip connections for both layers. For an input  $H^{(l)}$ , the (l+1)-th self-attention block works as follows:

$$\mathcal{A}^h = \operatorname{softmax}\left(\frac{H^{(l)}W_Q^{l,h}(H^{(l)}W_K^{l,h})^{\top}}{\sqrt{d}}\right); \qquad (7)$$

$$H^{(l+1)} = H^{(l)} + \sum_{i=1}^{B} \mathcal{A}^h H^{(l)} W_V^{l,h} W_O^{l,h}, \tag{8}$$

where  $\mathcal{A}^h$  is the attention matrix, B is the total number of attention heads, d is the dimension size,  $W_Q^{l,h}$ ,  $W_K^{l,h}$ , and  $W_V^{l,h}$  are learnable transformation matrices. To generalize Transformer to graph data, the positional encodings are indispensable for encoding topological and geometric information [41], [45]. Some representative methods graph

transformers are Graphormer [41], Transformer-M [45], and Equiformer [44].

#### 2.5 Generative Methods

In this subsection, we summarize the popular generative methods for structure-based drug design tasks, including autoregressive models, flow models, variational autoencoders, diffusion models, and some other methods.

# 2.5.1 Autoregressive Models (ARs)

Typically, the data point x can be factorized into a set of subcomponents  $\{x_0, x_1, \cdots, x_{d-1}\}$ , where d is the total number of subcomponents. For example, subcomponents can be pixels in images and nodes and edges in graphs. The subcomponents may have complicated underlying dependencies, which makes the direct generation of x very challenging. With predefined or learned orders, the autoregressive models factorize the joint distribution of x into the product of x subcomponent likelihoods as follows:

$$p(\mathbf{x}) = \prod_{i=1}^{d} p(x_i|x_1, x_2, ..., x_{i-1}).$$
 (9)

In the generation process, the autoregressive models generate  $\boldsymbol{x}$  in a sequential manner: the next subcomponent is predicted based on the previously generated subcomponents in each step.

#### 2.5.2 Flow Models

A flow model aims to learn a parameterized invertible function between the data point variable x and the latent variable z:  $f: z \in \mathbb{R}^d \to x \in \mathbb{R}^d$ . The latent distribution p(z) is a pre-defined probability distribution, *e.g.*, a Gaussian distribution. The data distribution p(x) is unknown. But given a data point x, its likelihood can be computed with the change-of-variable theorem:

$$p(x) = p(z) \left| \det \left( \frac{df^{-1}(x)}{dx} \right) \right|,$$
 (10)

where  $\det(\cdot)$  is the matrix determinant and  $\frac{df^{-1}(x)}{dx}$  is the Jacobian matrix.

In the sampling process, a latent variable z is first sampled from the pre-defined latent distribution p(z)). Then the corresponding data point x is obtained by performing the feedforward transformation x = f(z). Therefore, f needs to be inevitable, and the computation of  $\det J$  should be tractable for the training and sampling efficiency. A common choice is the affine coupling layers [47], [48] where the computation of  $\det J$  is very efficient because J is an upper triangular matrix.

# 2.5.3 Variational Autoencoders (VAEs)

Variational autoencoders (VAEs) [49] estimate and maximize the evidence lower bound (ELBO) of p(x). VAEs introduce the latent variable z and the loglikelihood of x can be expressed as:

$$\log p(\mathbf{x}) = \log \int_{\mathbf{z}} p(\mathbf{z}) p(\mathbf{x}|\mathbf{z}) d\mathbf{z}$$
(11)

$$\geq \mathbb{E}_{q(\boldsymbol{z}|\boldsymbol{x})} \big[ \log p(\boldsymbol{x}|\boldsymbol{z}) \big] - D_{KL}(q(\boldsymbol{z}|\boldsymbol{x})||p(\boldsymbol{z})) \quad (12)$$

$$\triangleq$$
 ELBO. (13)

Here, p(z) represents the prior distribution of x. For tractable calculation, parameterized encoder q(z|x) is usually used to approximate p(z|x), also known as the variational inference technique. The first term of ELBO is reconstruction loss which quantifies the information loss of reconstructing x from latent representations. The standard Gaussian prior  $p(z) \sim \mathcal{N}(0,I)$  typically leads to meansquared error (MSE) loss for the first term. The second term of ELBO is the KL-divergence term ensuring that our learned distribution q(z|x) is similar to the true prior distribution.

# 2.5.4 Diffusion models

Diffusion models [50], [51] are a class of generative models inspired by non-equilibrium thermodynamics. Generally, diffusion models define a Markovian chain of random diffusion steps by slowly adding noise to the data and then learning the reverse of this process via neural networks to reconstruct data samples from noise distributions, e.g., isotropic Gaussian.

Let  $x_0 \sim p(x)$  denote the original data and  $x_t, t = 1, \cdot, T$  indicate a series of noised representations with the same dimension as  $x_0$ . The forward diffusion process can be expressed as:

$$q(\boldsymbol{x}_t|\boldsymbol{x}_{t-1}) = \mathcal{N}(\boldsymbol{x}_t; \sqrt{1-\beta_t}\boldsymbol{x}_{t-1}, \beta_t I), \tag{14}$$

where  $\beta_t \in (0,1)$  controls the strength of Gaussian noise added in each step. A desirable property of the diffusion process is that a closed form of the intermediate state can be obtained. Let  $\alpha_t = 1 - \beta_t$ , and  $\bar{\alpha}_t = \prod_{i=1}^t \alpha_i$ , we have:

$$q(\boldsymbol{x}_t|\boldsymbol{x}_0) = \mathcal{N}(\boldsymbol{x}_t; \sqrt{\bar{\alpha}_t}\boldsymbol{x}_0, (1 - \bar{\alpha}_t)I), \tag{15}$$

Another desirable property is that the reverse of the diffusion process, i.e., the denoising process, can also be computed in closed form when conditioned on  $x_0$  with Bayes theorem:

$$p_{\theta}(\boldsymbol{x}_{t-1}|\boldsymbol{x}_t) = \mathcal{N}(\boldsymbol{x}_{t-1}; \boldsymbol{\mu}_t(\boldsymbol{x}_0, \boldsymbol{x}_t), \widetilde{\beta}_t I), \tag{16}$$

where the parameters can be obtained analytically:

$$\mu_{t}(\boldsymbol{x}_{0}, \boldsymbol{x}_{t}) = \frac{\sqrt{\bar{\alpha}_{t-1}}\beta_{t}}{1 - \bar{\alpha}_{t}}\boldsymbol{x}_{0} + \frac{\sqrt{\alpha_{t}}(1 - \bar{\alpha}_{t-1})}{1 - \bar{\alpha}_{t}}\boldsymbol{x}_{t},$$

$$\widetilde{\beta}_{t} = \frac{1 - \bar{\alpha}_{t-1}}{1 - \bar{\alpha}_{t}}\beta_{t}.$$
(17)

Similar to variational autoencoders, the objective of diffusion models is to maximize the variational lower bound of the log-likelihood of p(x):

$$-\log p(\boldsymbol{x}) \leq \underbrace{KL[q(x_T|x_0)||p_{\theta}(x_T)]}_{\text{prior loss } \mathcal{L}_T} + \sum_{t=2}^{T} \underbrace{KL[q(x_{t-1}|x_t, x_0)||p_{\theta}(x_{t-1}|x_t)]}_{\text{diffusion loss } \mathcal{L}_{t-1}} - \underbrace{\mathbb{E}_q[\log p_{\theta}(x_0|x_1)]}_{\text{reconstruction loss } \mathcal{L}_0}.$$

Here  $\mathcal{L}_T$  is a constant and can be ignored, and  $\mathcal{L}_0$  is usually estimated with separate models [51], [52]. For  $\{\mathcal{L}_{t-1}\}_{t=2}^T$ , diffusion models adopt a neural network  $\epsilon_{\theta}$  to predict the noise. More specifically, we can reparameterize Equation 15 as  $\mathbf{x}_t = \sqrt{\bar{\alpha}_t}\mathbf{x}_0 + \sqrt{(1-\bar{\alpha}_t)}\epsilon_t$ ,  $\epsilon_t \sim \mathcal{N}(0,I)$ . The following simplified training objective is widely adopted:

$$\mathcal{L} = \mathbb{E}_t \left[ \| \epsilon_t - \epsilon_\theta(\boldsymbol{x}_t, t) \|^2 \right].$$

#### 2.6 Other Methods

Besides the generative methods discussed above, some other methods such as Reinforcement Learning (RL) [53], Genetic Algorithm (GA) [54], and Monte Carlo Tree Search (MCTS) [17], [42] are employed to explore the chemical space with desirable properties. Furthermore, inspired by molecular dynamics and fragment-based drug design, some novel methods based on virtual dynamics (VD) [55] and fragment-based molecule generation (Fragment) [56] are proposed.

## 3 Tasks of Structure-Based Drug Design

# 3.1 Binding Site Prediction

# 3.1.1 Problem Formulation

The protein surface refers to the external regions of proteins that interact with the environment and is usually represented as a continuous shape with geometric and chemical features. Binding site prediction based on protein surface representations lays the foundation of other SBDD tasks such as binding pose generation and *de novo* ligand generation. Formally, denote the target protein surface as  $\mathcal{S}$  (e.g., mesh/point cloud), the objective is to learn a predictive model  $f(\mathcal{S})$  that outputs the probability of each point on the surface to be the binding site.

# 3.1.2 Representative Works

The Molecular Surface Interaction Fingerprinting (MaSIF) [13] method pioneered the use of 3D mesh-based geometric deep learning to predict protein interaction sites. However, MaSIF is limited by the reliance on precomputed meshes, handcrafted features, and significant computation time. dMaSIF [57] extend MaSIF and proposes an efficient end-to-end prediction framework based on 3D point cloud representations of protein. Furthermore, some recent works model protein surfaces as 3D graphs and design GNN [59] or Graph Transformer-based methods [58] for efficient and precise binding site prediction.

#### 3.1.3 Datasets

**Protein Data Bank (PDB)** [99] contains 3D structural protein data typically obtained by X-ray crystallography, NMR spectroscopy, or cryo-electron microscopy.

**Dockground** [100] provides a comprehensive set of proteinprotein docking complexes extracted from PDB.

## 3.1.4 Evaluation Metrics

As there is typically no threshold for the classification, **ROC-AUC** is widely used for the evaluation.

# 3.2 Binding Pose Generation

# 3.2.1 Problem Formulation

Predicting how the ligand molecule binds to the target protein target is a fundamental problem in drug discovery and has broad applications in virtual screening and drug engineering. Formally, denote the target protein structure as  $\mathcal{P}$ , the ligand molecular 2D-graph as G, and the 3D structure of ligand as R, the objective is to learn a model  $p(R|G,\mathcal{P})$  for ligand 3D structure prediction.

TABLE 1 Summary of structure-based drug design models with geometric deep learning reviewed in this paper.

Task	Model	Input	Output	Method
Binding site prediction	MaSIF [13] dMaSIF [57]	Protein Surface Protein Surface	Binding Site Probability Binding Site Probability	CNN CNN
	PeSTo [58]	Protein 3D-Graph	Binding Site Probability	Transformer
	ScanNet [59] PocketMiner [60] PIPGCN [61] EquiPocket [62] NodeCoder [63]	Protein 3D-Graph Protein 3D-Graph Protein 3D-Graph Protein 3D-Graph Protein 3D-Graph	Binding Site Probability Binding Site Probability Binding Site Probability Binding Site Probability Binding Site Probability	GNN GNN GNN GNN GNN
	DeepSite [30] PUResNet [31]	Protein Grid Protein Grid	Binding Site Probability Binding Site Probability	3DCNN 3DCNN
Binding pose generation	EquiBind [25]	Ligand 2D-Graph+Protein 3D-Graph	Complex 3D-Graph	Keypoint Align
	DeepDock [64] TankBind [65] EDM-Dock [66]	Ligand 2D-Graph+Protein Surface Ligand 2D-Graph+Protein 3D-Graph Ligand 2D-Graph+Protein 3D-Graph	Complex 3D-Graph Complex 3D-Graph Complex 3D-Graph	Dist. Pred. Dist. Pred. Dist. Pred.
	DPL [65] DiffDock [14] NeuralPLexer [67]	Ligand 2D-Graph+Protein Sequence Ligand 2D-Graph+Protein 3D-Graph Ligand 2D-Graph+Protein Sequence	Complex 3D-Graph Complex 3D-Graph Complex 3D-Graph	Diffusion Diffusion Diffusion
	E3Bind [68] DeepRMSD [69] 3T [70]	Ligand 2D-Graph+Protein 3D-Graph Ligand 2D-Graph+Protein 3D-Graph Ligand 2D-Graph+Protein 3D-Graph	Complex 3D-Graph Complex 3D-Graph Complex 3D-Graph	Iterative Update Iterative Update Iterative Update
Binding affinity prediction	SIGN [17] PIGNet [71] HOLOPROT [72] PLIG [73] PaxNet [74] IGN [75] GIGN [76] MBP [77]	Complex 3D-Graph Complex 3D-Graph+Surface Complex 3D-Graph Complex 3D-Graph Complex 3D-Graph Complex 3D-Graph Complex 3D-Graph Complex 3D-Graph	Binding Affinity Binding Affinity Binding Affinity Binding Affinity Binding Affinity Binding Affinity Binding Affinity Binding Affinity	GNN GNN GNN GNN GNN GNN GNN GNN
	Pafnucy [78] DeepAtom [79] RoseNet [80] IEConv [81] SGCNN [82]	Complex 3D-Grid Complex 3D-Grid Complex 3D-Grid Complex 3D-Graph Complex 3D-Graph	Binding Affinity Binding Affinity Binding Affinity Binding Affinity Binding Affinity	CNN CNN CNN CNN CNN
	Fusion [83]	Complex 3D-Grid+3D-Graph	Binding Affinity	CNN + GNN
de novo ligand generation	AutoGrow [84] RGA [54]	Pocket 3D-Graph Pocket 3D-Graph	Ligand 3D-Graph Ligand 3D-Graph	GA GA
	ligan [85] Relation [86] Squid [87]	Pocket Grid Pocket Grid Target Shape Point Cloud	Ligand 3D-Graph Ligand Smiles Ligand 3D-Graph	VAE VAE VAE+Fragment
	DeepLigBuilder [17] DeepLigBuilder+ [42]	Pocket 3D-Graph Pocket 3D-Graph	Ligand 3D-Graph Ligand 3D-Graph	MCTS+RL MCTS+RL
	3DSBDD [2] Pocket2Mol [15] DESERT [88] PrefixMol [89] FLAG [56] DrugGPS [90] Lingo3DMol [91]	Pocket 3D-Graph Pocket 3D-Graph Pocket Grid Pocket 3D-Graph Pocket 3D-Graph Pocket 3D-Graph Pocket 3D-Graph Pocket 3D-Graph	Ligand 3D-Graph Ligand 3D-Graph Ligand 3D-Graph Ligand Smiles Ligand 3D-Graph Ligand 3D-Graph Ligand 3D-Graph	AR AR AR AR AR+Fragment AR+Fragment AR+Fragment
	GraphBP [92] MolCode [93] GraphVF [94] SENF [95]	Pocket 3D-Graph Pocket 3D-Graph Pocket 3D-Graph Pocket 3D-Graph	Ligand 3D-Graph Ligand 3D-Graph Ligand 3D-Graph Ligand 3D-Graph	Flow Flow Flow+Fragment Flow
	DiffSBDD [1] TargetDiff [55] DiffBP [96]	Pocket 3D-Graph Pocket 3D-Graph Pocket 3D-Graph	Ligand 3D-Graph Ligand 3D-Graph Ligand 3D-Graph	Diffusion Diffusion Diffusion
	VD-Gen [55]	Pocket 3D-Graph	Ligand 3D-Graph	VD
Linker design	DeLinker [97] 3Dlinker [16]	Pocket 3D-Graph+Ligand Fragments Pocket 3D-Graph+Ligand Fragments	Ligand 2D-Graph Ligand 3D-Graph	VAE VAE
	PROTAC-INVENT [53]	Pocket 3D-Graph+Ligand Fragments	Ligand 3D-Graph	RL
	DiffLinker [98]	Pocket 3D-Graph+Ligand Fragments	Ligand 3D-Graph	Diffusion

# 3.2.2 Representative Works

Traditional docking methods rely on hand-designed scoring functions and insufficient conformation sampling. Recently, the docking problem has been tackled with geometric deep learning methods and achieves impressive progress. For example, EquiBind [25], an SE(3)-equivariant geometric deep learning model performs direct-shot prediction of both the receptor binding location (blind docking) and the ligand's bound pose by predicting and aligning pocket keypoints on both ligand and protein. TANKBind [65] improves over EquiBind by independently predicting a docking pose (interatomic distance matrix) for each possible pocket and then ranking them. Moreover, TANKBind proposes Trigonometry-Aware Neural networKs for binding structure prediction, which builds trigonometry constraints into the model. Instead of predicting the distance matrices, DiffDock [14] designs a diffusion generative model over the space of ligand poses for molecular docking; E3Bind [68] uses an equivariant network to iteratively updates the ligand pose. However, the protein structure is flexible and can undergo intrinsic or induced conformational changes [101], which is overlooked by the aforementioned methods. Some recent methods such as 3T [70] further consider the flexibility of the binding protein and achieve superior performance on protein-ligand complex structure prediction.

## 3.2.3 Datasets

**PDBBind** [102] is a subset of the Protein Data Bank (PDB) that contains experimentally measured 3D structures of protein-ligand complexes. The newest version, PDBBind v2020, contains 19 443 protein-ligand complexes with 3890 unique receptors and 15 193 unique ligands.

## 3.2.4 Evaluation Metrics

**Centroid Distance** calculates the distance between the averaged coordinates of the predicted and truly bound ligand atoms.

**Ligand Root Mean Square Deviation (L-RMSD)** is the mean squared error between the atoms of the predicted and bound ligands. Formally, let  $R \in \mathbb{R}^{n \times 3}$  and  $\hat{R} \in \mathbb{R}^{n \times 3}$  be the predicted and the ground truth ligand coordinates, where n is the number of atoms. The L-RMSD is obtained with:

L-RMSD
$$(R, \hat{R}) = \left(\frac{1}{n} \sum_{i=1}^{n} ||R_i - \hat{R}_i||^2\right)^{\frac{1}{2}},$$
 (18)

where  $R_i$  and  $\hat{R}_i$  denote the coordinate of the i-th atom. **Kabsch RMSD** is the lowest possible RMSD that can be obtained by the roto-translation transformation of the ligand. It first uses the Kabsch algorithm to superimpose the two structures and then calculates the RMSD score similar to Equation 18.

## 3.3 Binding Affinity Prediction

# 3.3.1 Problem Formulation

Protein-ligand binding affinity is a measurement of interaction strength and is a regression task. Accurate affinity prediction helps the design of effective drug molecules and plays an important role in SBDD. Formally, denoted the bound protein structure as  $\mathcal{P}$ , the bound ligand as  $\mathcal{L}$ , and the binding affinity as y, our target is to train a model  $f(\mathcal{P},\mathcal{L})=y$  for binding affinity prediction.

# 3.3.2 Representative Methods

The exploration of binding affinity prediction methods has a long-standing history. Early studies focused on utilizing empirical formulas [103] or designing handcrafted features coupled with traditional machine learning algorithms for binding affinity prediction [104]. Despite some advancements, these methods still exhibit limitations in terms of prediction accuracy and require significant efforts in feature design. Recent research has highlighted the application of geometric deep learning methods, which represent the protein-ligand complex structure as 3D grids or 3D graphs for processing and prediction. These approaches directly model the relationship between the complex's 3D structure and binding affinity using CNNs or GNNs. For example, given a complex structure, Pafnucy [78] extracts a 20 Å cubic box focused on the geometric center of the ligand and discretizes it into a  $21 \times 21 \times 21 \times 19$  grid with 1 Å resolution. A 3D-CNN is then employed to process the grid, treating it as a multi-channel 3D image. SIGN [17] converts the complex structure into a complex 3D graph and designs a structure-aware interactive graph neural network to capture 3D spatial information and global long-range interactions using polar-inspired graph attention layers in a semisupervised manner. Fusion [83] simultaneously utilizes the complex 3D grid representation and 3D graph to capture different characteristics of interactions. HOLOPROT [72] considers both complex structure and complex surface. MBP [77] introduces the first affinity pre-training framework, which involves training the model to predict the ranking of samples from the same bioassay. This pre-training is performed using a self-constructed ChEMBL-Dock dataset, which contains over 300k experimental affinity labels and about 2.8M docking generated complex structures. Overall, the geometric deep learning-based methods effectively capture the 3D structural information and show superior prediction accuracy.

## 3.3.3 Datasets

**PDBbind** [102] is the most commonly used dataset for binding affinity prediction. As previously mentioned, the latest version of the dataset consists of 19,443 complexes. Specifically, the dataset comprises three overlapping subsets: the general set (14,127 3D protein-ligand complexes), the refined set (5,316 complexes selected from the general set with higher quality), and the core set (290 complexes selected as the highest quality benchmark for testing). It is customary to train and validate models on either the general set or the refined set and subsequently evaluate them on the core set.

**CSAR-HiQ** [105] is another commonly used dataset, consisting of two subsets containing 176 and 167 complexes, respectively.

# 3.3.4 Evaluation Metrics

**Root Mean Square Error (RMSE)** and **Mean Absolute Error (MAE)** are widely used to quantify the errors between the predicted values and the ground-truth values [106]. These two metrics are the most direct evaluation metrics for prediction errors.

**Pearson's Correlation Coefficient (PCC)** [107] quantifies the linear correlation between the predicted values and

the ground-truth values. This metric serves as a means to evaluate prediction accuracy. Unlike RMSE and MAE, PCC is a normalized value ranging from -1 to 1, allowing for a standardized assessment of prediction accuracy.

**Spearman's Correlation Coefficient (SCC)** [108] quantifies the ranking correlation between predicted values and experimental values. It is calculated as the PCC between the rank values of the two variables. This metric is of great importance, as affinity prediction is frequently employed in virtual screening to identify molecules with the highest rankings.

# 3.4 de novo ligand generation

# 3.4.1 Problem Formulation

The goal of *de novo* ligand generation is to generate valid 3D molecular structures that can fit and bind to specific protein binding sites. *de novo* denotes that generating a molecule while no reference ligand molecule is given, i.e., generating molecules from scratch. Formally, let  $\mathcal P$  denote the protein structure and  $\mathcal G$  be the 3D ligand molecule, the objective is to learn a conditional generative model  $p(\mathcal G|\mathcal P)$  to capture the conditional distribution of protein-ligand pairs.

## 3.4.2 Representative Works

Early works on de novo ligand generation represents the target protein as 3D grid and employ 3D CNN as the encoder. For example, LiGAN [109] uses a conditional variational autoencoder trained on atomic density grid representations of protein-ligand structures for ligand generation. The molecular structures of ligands are then constructed by further atom fitting and bond inference from the generated atom densities. As a preliminary work, LiGAN does not satisfy the desirable equivariance property. The followup works represent the target protein and ligand as 3D graphs/point clouds and the equivariance is achieved by leveraging GNNs for context encoding. For example, 3DS-BDD [110] uses SchNet [111] to encode the 3D context of binding sites and estimate the probability density of atom's occurrences in 3D space. The atoms are sampled autoregressively until there is no room for new atoms. GraphBP [112] adopts the framework of normalizing flow [113] and constructs local coordinate systems to predict atom types and relative positions. Pocket2Mol [15] adopts the geometric vector perceptrons [114] and the vector-based neural network [115] as the context encoder. It also explicitly considers and predicts covalent chemical bonds. By leveraging the chemical priors of molecular fragments such as functional groups, FLAG [56] and DrugGPS [90] propose to generate ligand molecules fragment-by-fragment and yield more realistic substructures. Recently, motivated by the powerful generation capability of the Diffusion models, Diffusionbased methods such as DiffSBDD [1] and TargetDiff [55] are proposed for non-autoregressive ligand generation and achieve superior performance.

# 3.4.3 Datasets

**CrossDocked** dataset [116] is widely used in structure-based *de novo* ligand design [2], [15], which contains 22.5 million protein-molecule structures by crossdocking the Protein Data Bank [99]. After filtering out data points whose

binding pose RMSD is greater than 1 Å, a refined subset with around 180k data points is obtained. For the dataset split, mmseqs2 [117] is widely used to cluster data at 30% sequence identity, 100,000 protein-ligand pairs are randomly drawn for training and 100 proteins from remaining clusters for testing. 100 molecules for each protein pocket in the test set are sampled for the evaluation of generative models.

**Binding MOAD** [118] contains experimentally determined complexed protein-ligand structures. The dataset is filtered and split based on the proteins'enzyme commission number [119]. Specifically, the split is made to ensure different sets do not contain proteins from the same Enzyme Commission Number (EC Number) main class. Finally, there are 40,354 protein-ligand pairs for training and 130 pairs for testing.

#### 3.4.4 Evaluation Metrics

The following metrics are widely used in related works [2], [15], [56], [90], [112] to evaluate the qualities of the sampled molecules: (1) Validity is the percentage of chemically valid molecules among all generated molecules. A molecule is valid if it can be sanitized by RDkit [120]. (2) Vina Score measures the binding affinity between the generated molecules and the protein pockets. It can be calculate with traditional docking method such as AutoDock Vina [121], [122] or with trained CNN scoring functions [123]. Before calculating the vina score, the generated molecular structures are firstly refined by universal force fields [124]. (3) High Affinity is calculated as the percentage of pockets whose generated molecules have higher affinity to the references in the test set. (3) QED measures how likely a molecule is a potential drug candidate. (4) Synthetic Accessibility (SA) indicates the difficulty of drug synthesis (the score is normalized between 0 and 1 and higher values indicate easier synthesis). (5) LogP is the octanol-water partition coefficient (LogP values should be between -0.4 and 5.6 to be good drug candidates [125]). (6) Lipinski (Lip.) calculates how many rules the molecule obeys the Lipinski's rule of five [126]. (7) Sim. Train represents the Tanimoto similarity [127] with the most similar molecules in the training set. (8) Diversity (Div.) measures the diversity of generated molecules for a binding pocket (It is calculated as 1 - average pairwise Tanimoto similarities). (9) Time records the time cost to generate 100 valid molecules for a pocket.

# 3.5 Linker Design

#### 3.5.1 Problem Formulation

Most small molecular drugs work by binding to the target protein and inhibiting its activity. However, due to the complexity of diseases, some amino acids in target proteins may mutate, leading to weak binding affinity and drug falling off. To solve this problem, a recent drug mechanism named Proteolysis targeting chimera (PROTAC) is developed to inhibit the protein functions by prompting complete degradation of the target protein. Specifically, PROTAC contains two molecular fragments and a linker that links the fragments into a complete molecule. One fragment in PROTAC binds the target protein and the other fragment binds another molecule that can degrade the target protein. Due to the fact that PROTAC only requires high selectivity

in binding its targets instead of inhibiting the activity of the target protein, much attention is focused on repurposing previously ineffective inhibitor molecules as PROTAC for the next generation of drugs. One critical problem in PROTAC is linker design, which generates the linker conditioned on the given fragments and the target protein. Formally, denote the target protein as  $\mathcal{P}$ , the molecular fragments as  $\mathcal{F}$ , and the linker as  $\mathcal{L}$ , the objective is to learn a conditional generative model  $p(\mathcal{L}|\mathcal{F},\mathcal{P})$ .

## 3.5.2 Representative Works

DeLinker [97] uses the VAE architecture and autoregressively generates the atoms and edges of the linker. Only simple geometric information such as the relative distances and orientations is considered in DeLinker and the output is the 2D molecule graph. 3Dlinker [16] can further generate the 3D molecule structure and does not require specifying the anchor atoms, i.e., the atoms of fragments for linking. PROTAC-INVENT [53] jointly trains reinforcement learning to bias the generation of PROTAC structures toward predefined 2D and 3D-based properties. However, dinker design depends on the structural information of the target protein, which is overlooked in the above methods. DiffLinker [98] designs a conditional diffusion-based model that generates molecular linkers for a set of input fragments conditioned on the target protein structure. Results show that the consideration of the target protein structure improves the binding affinity of the resulting PROTAC molecules.

#### 3.5.3 Datasets

Zinc [128] is a free database of commercially-available compounds for virtual screening. A subset of 250,000 molecules randomly selected by [129] is used for linker design. The dataset is preprocessed as follows: firstly, 3D conformers are generated using RDKit [120] and a reference 3D structure with the lowest energy conformation is selected for each molecule. Then, these molecules are fragmented by enumerating all double cuts of acyclic single bonds outside functional groups. The results are further filtered by the number of atoms in the linker and fragments, synthetic accessibility [130], ring aromaticity, and pan-assay interference compounds (PAINS) [131] criteria. As a result, a single molecule may yield different combinations of two fragments separated by a linker.

**CASF** [132] includes experimentally verified 3D conformations. The preprocessing procedure is the same as Zinc.

**GEOM** [133] is considered for real-world applications that require connecting more than two fragments with one or more linkers. The molecule are decomposed into three or more fragments with one or two linkers with a MMPA-based algorithm [134] and BRICS [135].

**Binding MOAD** [118] contains experimentally determined complexed protein-ligand structures. DiffLinker [98] uses Binding MOAD to further assess the ability to generate valid linkers given additional information about protein pockets. The preprocessing process is similar to GEOM.

# 3.5.4 Evaluation Metrics

The following metrics are widely used to evaluate linker design methods: (1) **Validity** is the percentage of chemically valid molecules among all generated molecules. (2)

Quantitative Estimation of Drug-likeness (QED) measures how likely a molecule is a potential drug candidate. (3) Synthetic Accessibility (SA) indicates the difficulty of drug synthesis. (4) Rings is the average number of rings in the linker. (5) Uniqueness measures the percentage of non-duplicate generated molecules. (6) Novelty calculates the ratio of generated molecules not in the training set. (7) Recovery records the percentage of the original molecules that were recovered by the generation process. (8) Root Mean Squared Deviation (RMSD) is calculated between the generated and real linker coordinates in the cases where true molecules are recovered. (9) RD<sub>scit</sub> [136], [137] evaluates the geometric and chemical similarity between the ground-truth and generated molecules.

# 4 CHALLENGES AND OPPORTUNITIES

In this section, we summarize the challenges and opportunities we have in geometric deep learning for structure-based drug design from various perspectives, including problem formulation, data availability, evaluation metrics, prior knowledge, applications, etc.

# 4.1 Challenges

- Oversimplified Problem Formulation, the problem formulation for structure-based drug design tasks should respect real-world applications and physical/chemical laws. For example, most works on binding pose generation and *de novo* ligand generation assume that the target protein structure is fixed. However, the protein structure is flexible and can undergo intrinsic or induced conformational changes [101].
- Out-of-distribution Scenarios, most existing works overlook the out-of-distribution problem in model design and evaluation. Due to the limited size of datasets and the unreasonable dataset split, some works are over-optimistic of the proposed methods. For example, when unpredictable events like COVID-19 occur, the generative models are required to generate ligand molecules for new protein targets e.g., the main protease of SARS-CoV-2. Therefore, generalizable geometric deep learning models should be paid more attention for real-world applications.
- Lack of Fair Evaluation Metrics, this is related to how we define a good drug candidate. Although a series of evaluation metrics have been employed, they are still less satisfying. For example, the optimized models may exploit the shortcuts [138] in evaluation metrics and generate molecules with little practical usefulness.
- Lack of Large-scale Benchmark Datasets, though there are widely-used datasets and split for SBDD tasks, there is still a lack of large-scale fair benchmarks with high-quality data. For example, the refined set of PDBbind v2016 [102] used for training affinity prediction models only contains ~4k complexes. The CrossDocked dataset [116] used for *de novo* ligand design only contains 2,922 unique proteins and 13,780 unique ligand molecules. Obviously, the size of these datasets is much less than the size of drug candidates and proteins. Therefore, large-scale benchmarks with high-quality data are urgently required.

- Gap between SBDD Models and Real Applications, Researchers from the computer science/deep learning community focus on proposing general models while experts from biomedical areas care more about certain diseases and target proteins. Therefore, there are gaps between the developed SBDD models and real applications. As an interdisciplinary task, only close collaborations between researchers from both communities can benefit the real-world applications of geometric deep learning models on drug discovery.
- Lack of Wet Experiments Verification, though the designed drug candidates are evaluated with a series of metrics, it is still necessary to conduct wet-lab experiments to validate the effectiveness *in vivo* or *in vitro*. The obtained experimental results can further be used to rectify our model and create a closed loop between "dry computation" and "wet experiments".
- Lack of Interpretability, interpretability is an important yet challenging area for black-box deep learning models. In structure-based drug design tasks, the researchers may want to know why a protein-ligand complex has a high affinity or why an area on the protein surface is a promising binding site. The interpretability of SBDD models also helps researchers debug and update the model. There are some preliminary explorations to interpretability, e.g., [59], [139], [140]. However, the exploration of interpretable SBDD models is still limited overall.

# 4.2 Opportunities

- Leverage Multimodal data. The high-quality protein structure data is still limited, *e.g.*, the unique protein structures in CrossDocked and PDBbind are less than 10k. In contrast, UniRef [141] contains over 260 million protein sequences. According to biological domain knowledge, the sequences of amino acids in a protein determine its 3D structure and further its functions. Therefore, it is promising to incorporate protein language models [142], [143], [144] trained on protein sequence data for structure-based drug design. Moreover, text data describing protein functions [145] and proteomics [146] can be further incorporated into the SBDD model building.
- Extend to more Tasks. Essentially, this survey aims at giving a systematic review of geometric deep learning methods for structure-based drug design tasks, with a focus on small molecule drugs. Yet, most of the approaches in the discussed works are general and can be extended to other domains *e.g.*, antibody design [147], and crystal material generation [148].
- Incorporate more Domain Knowledge. Incorporating chemical and biomedical prior knowledge into the model building has demonstrated its effectiveness in a series of tasks. For instance, geometric symmetry is considered in equivariant neural networks; molecular fragments are considered to generate more realistic and valid molecules. In the future, geometric deep learning may benefit more by incorporating more domain knowledge.

- Build Standard Benchmark. Standard benchmarks can provide standardized dataset splits and evaluators that allow for easy and reliable comparison of different SBDD models in a unified manner.
- Consider later phases of drug development. Generally, structure-based drug design is in the early phases of drug discovery. There is a non-negligible gap between early-stage drug discovery and later phases in drug development [149], [150], leading to possible frustrations of drug candidates in clinical trials. Therefore, it would be helpful if we can consider the information and feedback from these later phases to develop better SBDD models.

# 5 CONCLUSION

In this survey, we provide a systematic review of geometric deep learning for structure-based drug design. We organize the existing works into five categories based on their tasks. For each task, we provide the problem formulation, summarize a bunch of representative works, and list the datasets and metrics for evaluation. Finally, we identify open challenges and opportunities in structure-based drug design. Still, a large number of novel methods and techniques are proposed each year. We hope this survey is able to help the readers quickly understand the limitations of current approaches and pave the way for the future of SBDD with geometric deep learning models.

## REFERENCES

- [1] A. Schneuing, Y. Du, C. Harris, A. Jamasb, I. Igashov, W. Du, T. Blundell, P. Lió, C. Gomes, M. Welling, M. Bronstein, and B. Correia, "Structure-based drug design with equivariant diffusion models," arXiv preprint arXiv:2210.13695, 2022.
- [2] S. Luo, J. Guan, J. Ma, and J. Peng, "A 3D generative model for structure-based drug design," in Thirty-Fifth Conference on Neural Information Processing Systems, 2021.
- [3] C. Isert, K. Atz, and G. Schneider, "Structure-based drug design with geometric deep learning," Current Opinion in Structural Biology, vol. 79, p. 102548, 2023.
- [4] J. Drenth, Principles of protein X-ray crystallography. Springer Science & Business Media, 2007.
- [5] J. Mitchell, J. B. W. Webber, and J. H. Strange, "Nuclear magnetic resonance cryoporometry," *Physics Reports*, vol. 461, no. 1, pp. 1–36, 2008.
- [6] R. Danev, H. Yanagisawa, and M. Kikkawa, "Cryo-electron microscopy methodology: current aspects and future directions," *Trends in biochemical sciences*, vol. 44, no. 10, pp. 837–848, 2019.
- [7] J. Jumper, R. Evans, A. Pritzel, T. Green, M. Figurnov, O. Ronneberger, K. Tunyasuvunakool, R. Bates, A. Žídek, A. Potapenko *et al.*, "Highly accurate protein structure prediction with alphafold," *Nature*, vol. 596, no. 7873, pp. 583–589, 2021.
- [8] A. Wlodawer and J. Vondrasek, "Inhibitors of hiv-1 protease: a major success of structure-assisted drug design," *Annual review of biophysics and biomolecular structure*, vol. 27, no. 1, pp. 249–284, 1909.
- [9] A. C. Anderson, "The process of structure-based drug design," *Chemistry & biology*, vol. 10, no. 9, pp. 787–797, 2003.
   [10] E. E. Rutenber and R. M. Stroud, "Binding of the anticancer drug
- [10] E. E. Rutenber and R. M. Stroud, "Binding of the anticancer drug zd1694 to e. coli thymidylate synthase: assessing specificity and affinity," *Structure*, vol. 4, no. 11, pp. 1317–1324, 1996.
  [11] K. Atz, F. Grisoni, and G. Schneider, "Geometric deep learning on
- [11] K. Atz, F. Grisoni, and G. Schneider, "Geometric deep learning on molecular representations," *Nature Machine Intelligence*, pp. 1–10, 2021.
- [12] V. G. Satorras, E. Hoogeboom, and M. Welling, "E(n) equivariant graph neural networks," *Proceedings of the 38th International Con*ference on Machine Learning, ICML, vol. 139, pp. 9323–9332, 2021.

- [13] P. Gainza, F. Sverrisson, F. Monti, E. Rodola, D. Boscaini, M. Bronstein, and B. Correia, "Deciphering interaction fingerprints from protein molecular surfaces using geometric deep learning," *Nature Methods*, vol. 17, no. 2, pp. 184–192, 2020.
- [14] G. Corso, H. Stärk, B. Jing, R. Barzilay, and T. Jaakkola, "Diffdock: Diffusion steps, twists, and turns for molecular docking," *ICLR*, 2023.
- [15] X. Peng, S. Luo, J. Guan, Q. Xie, J. Peng, and J. Ma, "Pocket2mol: Efficient molecular sampling based on 3d protein pockets," in International Conference on Machine Learning. PMLR, 2022, pp. 17 644–17 655.
- [16] Y. Huang, X. Peng, J. Ma, and M. Zhang, "3dlinker: An e (3) equivariant variational autoencoder for molecular linker design," ICML, 2022.
- [17] Y. Li, J. Pei, and L. Lai, "Structure-based de novo drug design using 3d deep generative models," *Chemical science*, vol. 12, no. 41, pp. 13 664–13 675, 2021.
- [18] C. L. Verlinde and W. G. Hol, "Structure-based drug design: progress, results and challenges," Structure, vol. 2, no. 7, pp. 577– 587, 1994.
- [19] P. M. Colman, "Structure-based drug design," Current opinion in structural biology, vol. 4, no. 6, pp. 868–874, 1994.
- [20] T. L. Blundell, "Structure-based drug design." Nature, vol. 384, no. 6604 Suppl, pp. 23–26, 1996.
- [21] G. Klebe, "Recent developments in structure-based drug design," Journal of molecular medicine, vol. 78, pp. 269–281, 2000.
- [22] L. G. Ferreira, R. N. Dos Santos, G. Oliva, and A. D. Andricopulo, "Molecular docking and structure-based drug design strategies," Molecules, vol. 20, no. 7, pp. 13384–13421, 2015.
- [23] R. Özçelik, D. van Tilborg, J. Jiménez-Luna, and F. Grisoni, "Structure-based drug discovery with deep learning," *Chem-BioChem*, p. e202200776, 2022.
- [24] M. Batool, B. Ahmad, and S. Choi, "A structure-based drug discovery paradigm," *International journal of molecular sciences*, vol. 20, no. 11, p. 2783, 2019.
- [25] H. Stärk, O.-E. Ganea, L. Pattanaik, R. Barzilay, and T. Jaakkola, "EquiBind: Geometric deep learning for drug binding structure prediction," arXiv preprint arXiv:2202.05146, 2022.
- [26] B. Jing, S. Eismann, P. Suriana, R. J. L. Townshend, and R. Dror, "Learning from protein structure with geometric vector perceptrons," in *International Conference on Learning Representations*, 2021. [Online]. Available: https://openreview.net/forum?id=1YLJDvSx6J4
- [27] D. Weininger, "SMILES, a chemical language and information system. 1. introduction to methodology and encoding rules," *Journal of chemical information and computer sciences*, vol. 28, no. 1, pp. 31–36, 1988.
- [28] Y. Du, T. Fu, J. Sun, and S. Liu, "Molgensurvey: A systematic survey in machine learning models for molecule design," *arXiv* preprint *arXiv*:2203.14500, 2022.
- [29] M. M. Bronstein, J. Bruna, Y. LeCun, A. Szlam, and P. Vandergheynst, "Geometric deep learning: going beyond euclidean data," *IEEE Signal Processing Magazine*, vol. 34, no. 4, pp. 18–42, 2017.
- [30] J. Jiménez, S. Doerr, G. Martínez-Rosell, A. S. Rose, and G. De Fabritiis, "Deepsite: protein-binding site predictor using 3d-convolutional neural networks," *Bioinformatics*, vol. 33, no. 19, pp. 3036–3042, 2017.
- [31] J. Kandel, H. Tayara, and K. T. Chong, "Puresnet: prediction of protein-ligand binding sites using deep residual neural network," *Journal of cheminformatics*, vol. 13, no. 1, pp. 1–14, 2021.
- [32] J. Han, Y. Rong, T. Xu, and W. Huang, "Geometrically equivariant graph neural networks: A survey," arXiv preprint arXiv:2202.07230, 2022.
- [33] K. T. Schütt, H. E. Sauceda, P.-J. Kindermans, A. Tkatchenko, and K.-R. Müller, "Schnet–a deep learning architecture for molecules and materials," *The Journal of Chemical Physics*, vol. 148, no. 24, p. 241722, 2018.
- [34] B. Jing, S. Eismann, P. Suriana, R. J. Townshend, and R. Dror, "Learning from protein structure with geometric vector perceptrons," arXiv preprint arXiv:2009.01411, 2020.
- [35] J. Klicpera, J. Groß, and S. Günnemann, "Directional message passing for molecular graphs," arXiv preprint arXiv:2003.03123, 2020.
- [36] J. Klicpera, S. Giri, J. T. Margraf, and S. Günnemann, "Fast and uncertainty-aware directional message passing for nonequilibrium molecules," arXiv preprint arXiv:2011.14115, 2020.

- [37] W. Huang, J. Han, Y. Rong, T. Xu, F. Sun, and J. Huang, "Equivariant graph mechanics networks with constraints," arXiv preprint arXiv:2203.06442, 2022.
- [38] Y. Liu, L. Wang, M. Liu, X. Zhang, B. Oztekin, and S. Ji, "Spherical message passing for 3d graph networks," *arXiv preprint* arXiv:2102.05013, 2021.
- [39] L. Wang, Y. Liu, Y. Lin, H. Liu, and S. Ji, "Comenet: Towards complete and efficient message passing for 3d molecular graphs," arXiv preprint arXiv:2206.08515, 2022.
- [40] J. Devlin, M. Chang, K. Lee, and K. Toutanova, "BERT: pretraining of deep bidirectional transformers for language understanding," in Proceedings of the 2019 Conference of the North American Chapter of the Association for Computational Linguistics: Human Language Technologies, NAACL-HLT 2019. Association for Computational Linguistics, 2019, pp. 4171–4186.
- [41] C. Ying, T. Cai, S. Luo, S. Zheng, G. Ke, D. He, Y. Shen, and T.-Y. Liu, "Do transformers really perform badly for graph representation?" Advances in Neural Information Processing Systems, vol. 34, 2021.
- [42] Y. Li, J. Pei, and L. Lai, "Synthesis-driven design of 3d molecules for structure-based drug discovery using geometric transformers," arXiv preprint arXiv:2301.00167, 2022.
- [43] Y. Rong, Y. Bian, T. Xu, W. Xie, Y. Wei, W. Huang, and J. Huang, "Self-supervised graph transformer on large-scale molecular data," in Advances in Neural Information Processing Systems, NeurIPS, 2020.
- [44] Y.-L. Liao and T. Smidt, "Equiformer: Equivariant graph attention transformer for 3d atomistic graphs," *arXiv* preprint *arXiv*:2206.11990, 2022.
- [45] S. Luo, T. Chen, Y. Xu, S. Zheng, T.-Y. Liu, L. Wang, and D. He, "One transformer can understand both 2d & 3d molecular data," arXiv preprint arXiv:2210.01765, 2022.
- [46] K. He, X. Zhang, S. Ren, and J. Sun, "Deep residual learning for image recognition," in *Proceedings of the IEEE conference on computer vision and pattern recognition*, 2016, pp. 770–778.
- [47] L. Dinh, D. Krueger, and Y. Bengio, "NICE: Non-linear independent components estimation," ICLR (Workshop), 2015.
- [48] L. Dinh, J. Sohl-Dickstein, and S. Bengio, "Density estimation using real NVP," arXiv preprint arXiv:1605.08803, 2016.
- [49] D. P. Kingma and M. Welling, "Auto-encoding variational bayes," International Conference on Learning Representations, 2013.
- [50] J. Sohl-Dickstein, E. Weiss, N. Maheswaranathan, and S. Ganguli, "Deep unsupervised learning using nonequilibrium thermodynamics," in *International Conference on Machine Learning*. PMLR, 2015, pp. 2256–2265.
- [51] J. Ho, A. Jain, and P. Abbeel, "Denoising diffusion probabilistic models," arXiv preprint arXiv:2006.11239, 2020.
- [52] L. Weng, "What are diffusion models?" lilianweng.github.io/lil-log, 2021. [Online]. Available: https://lilianweng.github.io/lil-log/ 2021/07/11/diffusion-models.html
- [53] H. Chen et al., "3d based generative protac linker design with reinforcement learning," 2023.
- [54] T. Fu, W. Gao, C. Coley, and J. Sun, "Reinforced genetic algorithm for structure-based drug design," Advances in Neural Information Processing Systems, vol. 35, pp. 12325–12338, 2022.
- [55] J. Guan, W. W. Qian, X. Peng, Y. Su, J. Peng, and J. Ma, "3d equivariant diffusion for target-aware molecule generation and affinity prediction," in *The Eleventh International Conference on Learning Representations*, 2023. [Online]. Available: https://openreview.net/forum?id=kJqXEPXMsE0
- [56] Z. Zhang, Y. Min, S. Zheng, and Q. Liu, "Molecule generation for target protein binding with structural motifs," in *The Eleventh International Conference on Learning Representations*, 2023.
- [57] F. Sverrisson, J. Feydy, B. E. Correia, and M. M. Bronstein, "Fast end-to-end learning on protein surfaces," in *Proceedings of the IEEE/CVF Conference on Computer Vision and Pattern Recognition*, 2021, pp. 15272–15281.
- [58] L. F. Krapp, L. A. Abriata, F. Cortés Rodriguez, and M. Dal Peraro, "Pesto: parameter-free geometric deep learning for accurate prediction of protein binding interfaces," *Nature Communications*, vol. 14, no. 1, p. 2175, 2023.
- [59] J. Tubiana, D. Schneidman-Duhovny, and H. J. Wolfson, "Scannet: an interpretable geometric deep learning model for structurebased protein binding site prediction," *Nature Methods*, vol. 19, no. 6, pp. 730–739, 2022.
- [60] A. Meller, M. D. Ward, J. H. Borowsky, J. M. Lotthammer, M. Kshirsagar, F. Oviedo, J. L. Ferres, and G. Bowman, "Predict-

- ing the locations of cryptic pockets from single protein structures using the pocketminer graph neural network," *Biophysical Journal*, vol. 122, no. 3, p. 445a, 2023.
- [61] A. Fout, J. Byrd, B. Shariat, and A. Ben-Hur, "Protein interface prediction using graph convolutional networks," *Advances in neural information processing systems*, vol. 30, 2017.
- [62] Y. Zhang, W. Huang, Z. Wei, Y. Yuan, and Z. Ding, "Equipocket: an e (3)-equivariant geometric graph neural network for ligand binding site prediction," arXiv preprint arXiv:2302.12177, 2023.
- [63] N. Abdollahi, S. A. M. Tonekaboni, J. Huang, B. Wang, and S. MacKinnon, "Nodecoder: a graph-based machine learning platform to predict active sites of modeled protein structures," arXiv preprint arXiv:2302.03590, 2023.
- [64] O. Méndez-Lucio, M. Ahmad, E. A. del Rio-Chanona, and J. K. Wegner, "A geometric deep learning approach to predict binding conformations of bioactive molecules," *Nature Machine Intelligence*, vol. 3, no. 12, pp. 1033–1039, 2021.
- [65] P. Nakata, Y. Mori, and S. Tanaka, "End-to-end protein-ligand complex structure generation with diffusion-based generative models," https://doi.org/10.1101/2022.12.20.521309, 2022.
- [66] M. R. Masters, A. H. Mahmoud, Y. Wei, and M. A. Lill, "Deep learning model for efficient protein–ligand docking with implicit side-chain flexibility," *Journal of Chemical Information and Model*ing, vol. 63, no. 6, pp. 1695–1707, 2023.
- [67] Z. Qiao, W. Nie, A. Vahdat, T. F. M. III, and A. Anand-kumar, "State-specific protein-ligand complex structure prediction with a multi-scale deep generative model," arXiv preprint arXiv:2209.15171, 2021.
- [68] Y. Zhang, H. Cai, C. Shi, B. Zhong, and J. Tang, "E3bind: An end-to-end equivariant network for protein-ligand docking," ICLR, 2023
- [69] Z. Wang, L. Zheng, S. Wang, M. Lin, Z. Wang, A. W.-K. Kong, Y. Mu, Y. Wei, and W. Li, "A fully differentiable ligand pose optimization framework guided by deep learning and a traditional scoring function," *Briefings in Bioinformatics*, vol. 24, no. 1, p. bbac520, 2023.
- [70] J. P. Mailoa, Z. Ye, J. Qiu, C.-Y. Hsieh, and S. Zhang, "Protein-ligand complex generator & drug screening via tiered tensor transform," arXiv preprint arXiv:2301.00984, 2023.
- [71] S. Moon, W. Zhung, S. Yang, J. Lim, and W. Y. Kim, "Pignet: a physics-informed deep learning model toward generalized drugtarget interaction predictions," *Chemical Science*, vol. 13, no. 13, pp. 3661–3673, 2022.
- [72] V. R. Somnath, C. Bunne, and A. Krause, "Multi-scale representation learning on proteins," Advances in Neural Information Processing Systems, vol. 34, pp. 25 244–25 255, 2021.
- [73] M. A. Moesser, D. Klein, F. Boyles, C. M. Deane, A. Baxter, and G. M. Morris, "Protein-ligand interaction graphs: Learning from ligand-shaped 3d interaction graphs to improve binding affinity prediction," bioRxiv, pp. 2022–03, 2022.
- [74] S. Zhang, Y. Liu, and L. Xie, "Efficient and accurate physics-aware multiplex graph neural networks for 3d small molecules and macromolecule complexes," arXiv preprint arXiv:2206.02789, 2022
- [75] D. Jiang, C.-Y. Hsieh, Z. Wu, Y. Kang, J. Wang, E. Wang, B. Liao, C. Shen, L. Xu, J. Wu et al., "Interactiongraphnet: A novel and efficient deep graph representation learning framework for accurate protein-ligand interaction predictions," *Journal of medicinal chemistry*, vol. 64, no. 24, pp. 18 209–18 232, 2021.
- [76] Z. Yang, W. Zhong, Q. Lv, T. Dong, and C. Yu-Chian Chen, "Geometric interaction graph neural network for predicting protein-ligand binding affinities from 3d structures (gign)," The Journal of Physical Chemistry Letters, vol. 14, no. 8, pp. 2020–2033, 2023.
- [77] J. Yan, Z. Ye, Z. Yang, C. Lu, S. Zhang, Q. Liu, and J. Qiu, "Multi-task bioassay pre-training for protein-ligand binding affinity prediction," arXiv preprint arXiv:2306.04886, 2023.
- [78] M. M. Stepniewska-Dziubinska, P. Zielenkiewicz, and P. Siedlecki, "Development and evaluation of a deep learning model for protein-ligand binding affinity prediction," *Bioinformatics*, vol. 34, pp. 3666 – 3674, 2018.
- [79] Y. Li, M. A. Rezaei, C. Li, X. Li, and D. O. Wu, "Deepatom: A framework for protein-ligand binding affinity prediction," 2019 IEEE International Conference on Bioinformatics and Biomedicine (BIBM), pp. 303–310, 2019.
- [80] H. Hassan-Harrirou, C. Zhang, and T. Lemmin, "Rosenet: Improving binding affinity prediction by leveraging molecular me-

- chanics energies with an ensemble of 3d convolutional neural networks," *Journal of chemical information and modeling*, 2020.
- [81] P. Hermosilla, M. Schäfer, M. Lang, G. Fackelmann, P. P. Vázquez, B. Kozlíková, M. Krone, T. Ritschel, and T. Ropinski, "Intrinsicextrinsic convolution and pooling for learning on 3d protein structures," arXiv preprint arXiv:2007.06252, 2020.
- [82] R. Lu, J. Wang, P. Li, Y. Li, S. Tan, Y. Pan, H. Liu, P. Gao, G. Xie, and X. Yao, "Improving drug-target affinity prediction via feature fusion and knowledge distillation," *Briefings in Bioinformatics*, vol. 24, no. 3, p. bbad145, 2023.
- [83] D. Jones, H. Kim, X. Zhang, A. T. Zemla, G. Stevenson, W. F. D. Bennett, D. A. Kirshner, S. E. Wong, F. C. Lightstone, and J. E. Allen, "Improved protein-ligand binding affinity prediction with structure-based deep fusion inference," *Journal of chemical information and modeling*, 2020.
- [84] J. O. Spiegel and J. D. Durrant, "Autogrow4: an open-source genetic algorithm for de novo drug design and lead optimization," Journal of cheminformatics, vol. 12, no. 1, pp. 1–16, 2020.
- [85] T. Masuda, M. Ragoza, and D. R. Koes, "Generating 3d molecular structures conditional on a receptor binding site with deep generative models," arXiv preprint arXiv:2010.14442, 2020.
- [86] M. Wang, C.-Y. Hsieh, J. Wang, D. Wang, G. Weng, C. Shen, X. Yao, Z. Bing, H. Li, D. Cao et al., "Relation: A deep generative model for structure-based de novo drug design," *Journal of Medicinal Chemistry*, vol. 65, no. 13, pp. 9478–9492, 2022.
- [87] K. Adams and C. W. Coley, "Equivariant shape-conditioned generation of 3d molecules for ligand-based drug design," ICLR, 2023.
- [88] S. Long, Y. Zhou, X. Dai, and H. Zhou, "Zero-shot 3d drug design by sketching and generating," arXiv preprint arXiv:2209.13865, 2022.
- [89] Z. Gao, Y. Hu, C. Tan, and S. Z. Li, "Prefixmol: Target-and chemistry-aware molecule design via prefix embedding," arXiv preprint arXiv:2302.07120, 2023.
- [90] Z. Zhang and Q. Liu, "Learning subpocket prototypes for generalizable structure-based drug design," in *The Fortieth International Conference on Machine Learning*, 2023.
- [91] L. Wang, Z. Lin, Y. Zhu, R. Bai, W. Feng, H. Wang, J. Zhou, W. Peng, B. Huang, and W. Zhou, "Lingo3dmol: Generation of a pocket-based 3d molecule using a language model," arXiv preprint arXiv:2305.10133, 2023.
- [92] M. Liu, Y. Luo, K. Uchino, K. Maruhashi, and S. Ji, "Generating 3d molecules for target protein binding," in *International Conference* on Machine Learning, 2022.
- [93] Z. Zhang, Q. Liu, C.-K. Lee, C.-Y. Kim, and E. Chen, "An equivariant generative framework for molecular graph-structure co-design," bioRxiv, pp. 2023–04, 2023.
- [94] F. Sun, Z. Zhan, H. Guo, M. Zhang, and J. Tang, "Graphvf: Controllable protein-specific 3d molecule generation with variational flow," arXiv preprint arXiv:2304.12825, 2023.
- [95] E. Rozenberg, E. Rivlin, and D. Freedman, "Structure-based drug design via semi-equivariant conditional normalizing flows," in ICLR 2023 - Machine Learning for Drug Discovery workshop, 2023. [Online]. Available: https://openreview.net/forum?id= TY5iNiUSo-
- [96] H. Lin, Y. Huang, M. Liu, X. Li, S. Ji, and S. Z. Li, "Diffbp: Generative diffusion of 3d molecules for target protein binding," arXiv preprint arXiv:2211.11214, 2022.
- [97] F. Imrie, A. R. Bradley, M. van der Schaar, and C. M. Deane, "Deep generative models for 3d linker design," *Journal of chemical information and modeling*, vol. 60, no. 4, pp. 1983–1995, 2020.
- [98] I. Igashov, H. Stärk, C. Vignac, V. G. Satorras, P. Frossard, M. Welling, M. Bronstein, and B. Correia, "Equivariant 3dconditional diffusion models for molecular linker design," arXiv preprint arXiv:2210.05274, 2022.
- [99] H. M. Berman, J. Westbrook, Z. Feng, G. Gilliland, T. N. Bhat, H. Weissig, I. N. Shindyalov, and P. E. Bourne, "The protein data bank," *Nucleic acids research*, vol. 28, no. 1, pp. 235–242, 2000.
- [100] P. J. Kundrotas, I. Anishchenko, T. Dauzhenka, I. Kotthoff, D. Mnevets, M. M. Copeland, and I. A. Vakser, "Dockground: a comprehensive data resource for modeling of protein complexes," *Protein Science*, vol. 27, no. 1, pp. 172–181, 2018.
- [101] D. E. Koshland Jr, "The key–lock theory and the induced fit theory," Angewandte Chemie International Edition in English, vol. 33, no. 23-24, pp. 2375–2378, 1995.
- [102] Z. Liu, M. Su, L. Han, J. Liu, Q. Yang, Y. Li, and R. Wang, "Forging the basis for developing protein-ligand interaction scoring func-

- tions," Accounts of chemical research, vol. 50, no. 2, pp. 302–309, 2017.
- [103] I. A. Guedes, F. S. S. Pereira, and L. E. Dardenne, "Empirical scoring functions for structure-based virtual screening: Applications, critical aspects, and challenges," Frontiers in Pharmacology, vol. 9, 2018.
- [104] G. Bitencourt-Ferreira, C. Rizzotto, and W. F. de Azevedo Junior, "Machine learning-based scoring functions. development and applications with sandres." Current medicinal chemistry, 2020.
- [105] J. B. Dunbar, R. D. Smith, K. L. Damm-Ganamet, A. Ahmed, E. X. Esposito, J. Delproposto, K. Chinnaswamy, Y.-N. Kang, G. Kubish, J. E. Gestwicki, J. A. Stuckey, and H. A. Carlson, "Csar data set release 2012: Ligands, affinities, complexes, and docking decoys," *Journal of Chemical Information and Modeling*, vol. 53, pp. 1842 – 1852, 2013.
- [106] J. D. Durrant, S. Lindert, and J. A. McCammon, "Autogrow 3.0: an improved algorithm for chemically tractable, semi-automated protein inhibitor design," *Journal of Molecular Graphics and Modelling*, vol. 44, pp. 104–112, 2013.
- [107] K. Yeager, "Spss tutorials: Pearson correlation," University Libraries: Geneva, Switzerland, 2019.
- [108] P. Sedgwick, "Spearman's rank correlation coefficient," Bmj, vol. 349, 2014.
- [109] M. Ragoza, T. Masuda, and D. R. Koes, "Generating 3d molecules conditional on receptor binding sites with deep generative models," *Chemical science*, vol. 13, no. 9, pp. 2701–2713, 2022.
- [110] Y. Luo and S. Ji, "An autoregressive flow model for 3d molecular geometry generation from scratch," in *International Conference on Learning Representations*, 2021.
- [111] K. Schütt, P.-J. Kindermans, H. E. Sauceda Felix, S. Chmiela, A. Tkatchenko, and K.-R. Müller, "Schnet: A continuous-filter convolutional neural network for modeling quantum interactions," NeurIPS, vol. 30, 2017.
- [112] M. Liu, Y. Luo, K. Uchino, K. Maruhashi, and S. Ji, "Generating 3d molecules for target protein binding," ICML, 2022.
- [113] D. Rezende and S. Mohamed, "Variational inference with normalizing flows," in ICML. PMLR, 2015, pp. 1530–1538.
- [114] B. Jing, S. Eismann, P. N. Soni, and R. O. Dror, "Equivariant graph neural networks for 3d macromolecular structure," *ICML*, 2021.
- [115] C. Deng, O. Litany, Y. Duan, A. Poulenard, A. Tagliasacchi, and L. J. Guibas, "Vector neurons: A general framework for so (3)equivariant networks," in CVPR, 2021, pp. 12200–12209.
- [116] P. G. Francoeur, T. Masuda, J. Sunseri, A. Jia, R. B. Iovanisci, I. Snyder, and D. R. Koes, "Three-dimensional convolutional neural networks and a cross-docked data set for structure-based drug design," *Journal of Chemical Information and Modeling*, vol. 60, no. 9, pp. 4200–4215, 2020.
- [117] M. Steinegger and J. Söding, "Mmseqs2 enables sensitive protein sequence searching for the analysis of massive data sets," *Nature biotechnology*, vol. 35, no. 11, pp. 1026–1028, 2017.
- [118] L. Hu, M. L. Benson, R. D. Smith, M. G. Lerner, and H. A. Carlson, "Binding moad (mother of all databases)," Proteins: Structure, Function, and Bioinformatics, vol. 60, no. 3, pp. 333–340, 2005.
  [119] A. Bairoch, "The enzyme data bank," Nucleic acids research,
- [119] A. Bairoch, "The enzyme data bank," *Nucleic acids research* vol. 22, no. 17, pp. 3626–3627, 1994.
- [120] A. P. Bento, A. Hersey, E. Félix, G. Landrum, A. Gaulton, F. Atkinson, L. J. Bellis, M. De Veij, and A. R. Leach, "An open source chemical structure curation pipeline using rdkit," *Journal of Cheminformatics*, vol. 12, no. 1, pp. 1–16, 2020.
- [121] O. Trott and A. J. Olson, "AutoDock Vina: improving the speed and accuracy of docking with a new scoring function, efficient optimization, and multithreading," *Journal of computational chemistry*, vol. 31, no. 2, pp. 455–461, 2010.
- [122] A. Alhossary, S. D. Handoko, Y. Mu, and C.-K. Kwoh, "Fast, accurate, and reliable molecular docking with quickvina 2," *Bioinformatics*, vol. 31, no. 13, pp. 2214–2216, 2015.
- [123] M. Ragoza, J. Hochuli, E. Idrobo, J. Sunseri, and D. R. Koes, "Protein-ligand scoring with convolutional neural networks," *Journal of chemical information and modeling*, vol. 57, no. 4, pp. 942–957, 2017.
- [124] A. K. Rappé, C. J. Casewit, K. Colwell, W. A. Goddard III, and W. M. Skiff, "Uff, a full periodic table force field for molecular mechanics and molecular dynamics simulations," *Journal of the American chemical society*, vol. 114, no. 25, pp. 10024–10035, 1992.
- [125] A. K. Ghose, V. N. Viswanadhan, and J. J. Wendoloski, "A knowledge-based approach in designing combinatorial or medicinal chemistry libraries for drug discovery. 1. a qualitative and

- quantitative characterization of known drug databases," *Journal of combinatorial chemistry*, vol. 1, no. 1, pp. 55–68, 1999.
- [126] C. A. Lipinski, F. Lombardo, B. W. Dominy, and P. J. Feeney, "Experimental and computational approaches to estimate solubility and permeability in drug discovery and development settings," Advanced drug delivery reviews, vol. 64, pp. 4–17, 2012.
- [127] D. Bajusz, A. Rácz, and K. Héberger, "Why is tanimoto index an appropriate choice for fingerprint-based similarity calculations?" *Journal of cheminformatics*, vol. 7, no. 1, pp. 1–13, 2015.
- [128] T. Sterling and J. J. Irwin, "ZINC 15-ligand discovery for every-one," *Journal of chemical information and modeling*, vol. 55, no. 11, pp. 2324–2337, 2015.
- [129] R. Gómez-Bombarelli, J. N. Wei, D. Duvenaud, J. M. Hernández-Lobato, B. Sánchez-Lengeling, D. Sheberla, J. Aguilera-Iparraguirre, T. D. Hirzel, R. P. Adams, and A. Aspuru-Guzik, "Automatic chemical design using a data-driven continuous representation of molecules," ACS central science, 2018.
- [130] P. Ertl and A. Schuffenhauer, "Estimation of synthetic accessibility score of drug-like molecules based on molecular complexity and fragment contributions," *Journal of cheminformatics*, vol. 1, no. 1, p. 8, 2009.
- [131] J. B. Baell and G. A. Holloway, "New substructure filters for removal of pan assay interference compounds (pains) from screening libraries and for their exclusion in bioassays," *Journal* of medicinal chemistry, vol. 53, no. 7, pp. 2719–2740, 2010.
- [132] M. Su, Q. Yang, Y. Du, G. Feng, Z. Liu, Y. Li, and R. Wang, "Comparative assessment of scoring functions: the casf-2016 update," *Journal of chemical information and modeling*, vol. 59, no. 2, pp. 895–913, 2018.
- [133] S. Axelrod and R. Gomez-Bombarelli, "Geom, energy-annotated molecular conformations for property prediction and molecular generation," *Scientific Data*, vol. 9, no. 1, p. 185, 2022.
- [134] A. G. Dossetter, E. J. Griffen, and A. G. Leach, "Matched molecular pair analysis in drug discovery," *Drug Discovery Today*, vol. 18, no. 15-16, pp. 724–731, 2013.
- [135] J. Degen, C. Wegscheid-Gerlach, A. Zaliani, and M. Rarey, "On the art of compiling and using drug-like chemical fragment spaces," *ChemMedChem: Chemistry Enabling Drug Discovery*, vol. 3, no. 10, pp. 1503–1507, 2008.
- [136] S. Putta, G. A. Landrum, and J. E. Penzotti, "Conformation mining: an algorithm for finding biologically relevant conformations," *Journal of medicinal chemistry*, vol. 48, no. 9, pp. 3313–3318, 2005
- [137] G. A. Landrum, J. E. Penzotti, and S. Putta, "Feature-map vectors: a new class of informative descriptors for computational drug discovery," *Journal of computer-aided molecular design*, vol. 20, pp. 751–762, 2006.
- [138] R. Geirhos, J.-H. Jacobsen, C. Michaelis, R. Zemel, W. Brendel, M. Bethge, and F. A. Wichmann, "Shortcut learning in deep neural networks," *Nature Machine Intelligence*, vol. 2, no. 11, pp. 665–673, 2020.
- [139] H. He, G. Chen, and C. Y.-C. Chen, "Nhgnn-dta: A node-adaptive hybrid graph neural network for interpretable drug-target binding affinity prediction," *Bioinformatics*, p. btad355, 2023.
- [140] H. T. Rube, C. Rastogi, S. Feng, J. F. Kribelbauer, A. Li, B. Becerra, L. A. Melo, B. V. Do, X. Li, H. H. Adam et al., "Prediction of protein-ligand binding affinity from sequencing data with interpretable machine learning," Nature Biotechnology, vol. 40, no. 10, pp. 1520–1527, 2022.
- [141] B. E. Suzek, H. Huang, P. McGarvey, R. Mazumder, and C. H. Wu, "Uniref: comprehensive and non-redundant uniprot reference clusters," *Bioinformatics*, vol. 23, no. 10, pp. 1282–1288, 2007.
- [142] N. Ferruz, S. Schmidt, and B. Höcker, "Protgpt2 is a deep unsupervised language model for protein design," *Nature communications*, vol. 13, no. 1, p. 4348, 2022.
- [143] Z. Lin, H. Akin, R. Rao, B. Hie, Z. Zhu, W. Lu, N. Smetanin, A. dos Santos Costa, M. Fazel-Zarandi, T. Sercu, S. Candido et al., "Language models of protein sequences at the scale of evolution enable accurate structure prediction," bioRxiv, 2022.
- [144] A. Madani, B. McCann, N. Naik, N. S. Keskar, N. Anand, R. R. Eguchi, P.-S. Huang, and R. Socher, "Progen: Language modeling for protein generation," arXiv preprint arXiv:2004.03497, 2020.
- [145] M. Xu, X. Yuan, S. Miret, and J. Tang, "Protst: Multi-modality learning of protein sequences and biomedical texts," arXiv preprint arXiv:2301.12040, 2023.

- [146] B. Aslam, M. Basit, M. A. Nisar, M. Khurshid, and M. H. Rasool, "Proteomics: technologies and their applications," *Journal of chromatographic science*, pp. 1–15, 2016.
- [147] X. Kong, W. Huang, and Y. Liu, "Conditional antibody design as 3d equivariant graph translation," arXiv preprint arXiv:2208.06073, 2022.
- [148] T. Xie, X. Fu, O.-E. Ganea, R. Barzilay, and T. Jaakkola, "Crystal diffusion variational autoencoder for periodic material generation," arXiv preprint arXiv:2110.06197, 2021.
- [149] T. Fu, K. Huang, C. Xiao, L. M. Glass, and J. Sun, "HINT: Hierarchical interaction network for clinical-trial-outcome predictions," *Cell Patterns*, p. 100445, 2022.
- [150] T. Fu, C. Xiao, C. Qian, L. M. Glass, and J. Sun, "Probabilistic and dynamic molecule-disease interaction modeling for drug discovery," in *Proceedings of the 27th ACM SIGKDD Conference* on Knowledge Discovery & Data Mining, 2021, pp. 404–414.